Materials Characterization 114 (2016) 151–156

Contents lists available at ScienceDirect

Materials Characterization

journal homepage: www.elsevier.com/locate/matchar

Phase transformations in a Cu−−Cr alloy induced by high pressure torsion

Anna Korneva [a,*], Boris Straumal [b,c,d], Askar Kilmametov [c], Robert Chulist [a], Piotr Straumal [d], Paweł Zięba [a]

[a] Institute of Metallurgy and Materials Science, Polish Academy of Sciences, Reymonta St. 25, 30-059 Cracow, Poland
[b] Institute of Solid State Physics, Russian Academy of Sciences, Ac. Ossipzn Str. 2, Chernogolovka 142432, Russia
[c] Institut für Nanotechnologie, Karlsruher Institut für Technologie, Hermann-von-Helmholtz-Platz 1, 76344 Eggenstein-Leopoldshafen, Germany
[d] Laboratory of Hybrid Nanomaterials, National University of Science and Technology «MISIS», Leninskii prosp. 4, 119049 Moscow, Russia

ARTICLE INFO

Article history:
Received 12 January 2016
Received in revised form 23 February 2016
Accepted 24 February 2016
Available online 27 February 2016

Keywords:
Cu—Cr alloy
High pressure torsion
Phase transformations
Microhardness

ABSTRACT

Phase transformations induced by high pressure torsion (HPT) at room temperature in two samples of the Cu-0.86 at.% Cr alloy, pre-annealed at 550 °C and 1000 °C, were studied in order to obtain two different initial states for the HPT procedure. Observation of microstructure of the samples before HPT revealed that the sample annealed at 550 °C contained two types of Cr precipitates in the Cu matrix: large particles (size about 500 nm) and small ones (size about 70 nm). The sample annealed at 1000 °C showed only a little fraction of Cr precipitates (size about 2 μm). The subsequent HPT process resulted in the partial dissolution of Cr precipitates in the first sample and dissolution of Cr precipitates with simultaneous decomposition of the supersaturated solid solution in another. However, the resulting microstructure of the samples after HPT was very similar from the standpoint of grain size, phase composition, texture analysis and hardness measurements.

1. Introduction

Cu—Cr alloys are promising precipitation-hardening materials due to the combination of high strength, high electrical and thermal conductivity and excellent fatigue resistance [1–3]. Generally, the alloys with good electrical conductivity produced with conventional metallurgical processes contain less than 1 at.% chromium [3,4]. The precipitation hardening (solution treatment, quenching and aging) leads to good electrical conductivity and high level of strength. However, even greater strength of copper alloys is required due to the rapid development of electronic industry, and this can be achieved by the application of severe plastic deformation (SPD), which provides an intensive grain refinement. Recently, there have been many works dedicated to the study of influence of SPD (such as hot-rolling-quenching process [1], mechanical alloying [5], or equal-channel angular pressing [6–8]) on the grain refinement, strength and electrical conductivity of Cu—Cr alloys. The SPD process not only induces strong grain refinement but frequently leads to the phase transformations such as dissolution of phases [9–11], formation [12,13] or the decomposition of supersaturated solid solution [14–16], decomposition of amorphous phase with the formation of nanocrystals [17,18], allotropic phase transformation [19,20] etc. The study of these phase transformations is an important aspect in understanding the influence of SPD on the microstructure and properties of materials. Therefore, the aim of the present work has been to examine the types and sequence of the phase transformations taking place in the Cu-0.86 at.% Cr alloy subjected to the high pressure torsion (HPT) deformation.

2. Experimental procedure

The Cu-0.86 at.% Cr alloy, in the form of cylindrical ingots, has been prepared from a high-purity 5 N Cu and 5 N Cr by vacuum induction melting. For the HPT processing, the 0.6 mm thick discs were cut from the as-cast ingots, then grinded and chemically etched. They were sealed into evacuated silica ampoules with a residual pressure of approximately $4\times^{10-4}$ Pa at room temperature. The samples were annealed at two different conditions: 550 °C for 2300 h and 1000 °C for 384 h in order to obtain two different initial states, and then quenched in water. The annealed samples were processed by the HPT at room temperature for five full rotations at a constant rotation speed of one rotation per minute and a pressure of 5 GPa using a computer controlled custom designed HPT device (W. Klement GmbH, Lang, Austria). The samples for the microstructure examination were cut from the HPT-processed discs at the distance of 3 mm from the sample center. For the metallographic investigations the samples were ground with SiC grinding paper, and sequentially polished with 6, 3, and 1 μm diamond pastes. The prior inspection of the obtained material was carried out on a Philips XL30 scanning electron microscope (SEM) equipped with a LINK ISIS energy-dispersive X-ray spectrometer (EDS) produced by Oxford Instruments. The crystallographic orientation of deformed samples was determined by means of electron backscatter diffraction (EBSD) analysis in the SEM, FEI Quanta 3D FEGSEM. The

* Corresponding author.
E-mail address: a.korniewa@imim.pl (A. Korneva).

http://dx.doi.org/10.1016/j.matchar.2016.02.017
1044-5803/

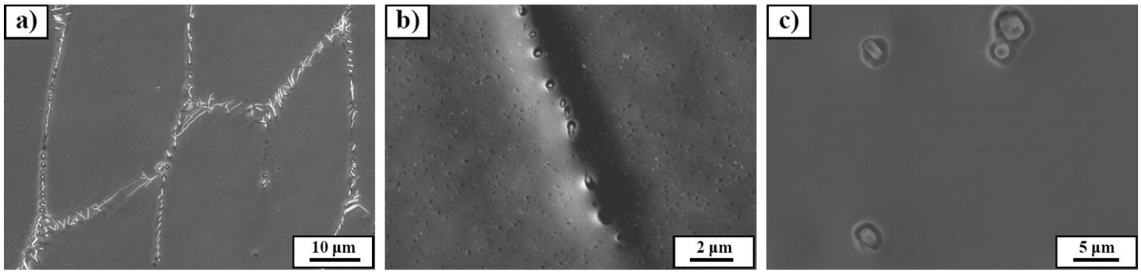

Fig. 1. SEM micrographs of the as cast Cu-0.86 at.% Cr alloy (a), annealed at 550 °C for 2300 h (b) and at 1000 °C for 384 h (c).

Table 1
Chromium content in the copper matrix and chromium precipitates measured by EDS on SEM or TEM in the samples before and after deformation, at.%.

Samples	Before HPT			After HPT		
	Matrix	Large precipitates	Small precipitates	Matrix	Large precipitates	Small precipitates
After annealing at 550 °C	0.1 ± 0.1 (TEM)	85.1 ± 1.7 (TEM)	86.7 ± 1.7 (TEM)	0.3 ± 0.1 (TEM)	39.2 ± 0.8 (TEM)	40.9 ± 0.8 (TEM)
After annealing at 1000 °C	0.8 ± 0.4 (SEM)	79.9 ± 1.6 (SEM)	–	0.7 ± 0.4 (SEM)	47.8 ± 1.0 (SEM)	45.8 ± 0.9 (TEM)

measurement step was 50 nm. The details of the phases, especially in nanoscale, were revealed using a TECNAI G2 FEG super TWIN (200 kV) transmission electron microscope (TEM) equipped with EDS system manufactured by EDAX. Thin foils for TEM observation were prepared by a twin-jet polishing technique using electrolyte D2 manufactured by Struers company. The X-ray diffraction patterns were obtained using Bragg–Brentano geometry in a powder diffractometer (Philips X'Pert) with Cu-Kα radiation. The hardness was measured with the Vickers method at the load of 100 μN using the CSM Instrument. The texture of the HPT deformed materials was measured with EBSD at the distance of 3 mm from the edge of the disc-shaped sample. The single orientation files composed of more than 3000 grains were used to calculate the orientation distribution function (ODF) and to ensure good grain statistics. For the ODF calculation Labotex software was applied [21].

3. Results and discussion

The microstructure of the Cu-0.86 at.% Cr alloy after casting contained crystals of a copper solid solution, on the boundaries of which the eutectic mixture of the copper solid solution and chromium precipitates was located (Fig. 1a). The annealing of the as-cast alloy at 550 °C resulted in the partial dissolution of the eutectics, so chromium precipitates of size about 500 nm were observed at the boundaries of the former Cu solid solution crystals. Additionally, small Cr particles with a size about 70 nm uniformly distributed in the Cu matrix were visible (Fig. 1b). The annealing of the as-cast alloy at 1000 °C led to the dissolution and coalescence of the chromium precipitates. Only a little fraction of Cr precipitates with size about 2 μm again uniformly distributed in the Cu matrix was observed (Fig. 1c). The grain size of Cu matrix in the both samples after annealing was more than 500 μm.

The EDS chemical composition analysis of the annealed samples was performed in the SEM in the case of large particles and in the TEM for the small ones. The analysis showed that the precipitates were enriched in chromium up to about 86 at.% while the matrix was almost pure copper (Table 1).

The X-ray diffraction patterns of the Cu-0.86 at.% Cr alloy after annealing and after HPT process are shown in Fig. 2. A very small (110) peak of Cr particles at the right side of the (111) Cu peak was visible after annealing at 550 °C, due to small content of chromium in the

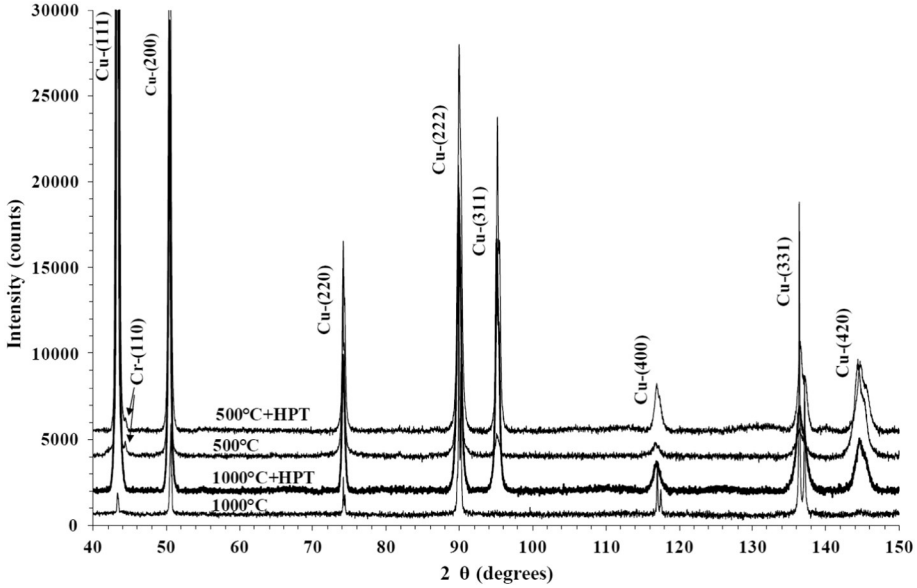

Fig. 2. X-ray diffraction patterns of the Cu-0.86 at.% Cr alloy after annealing at different temperatures and after HPT process.

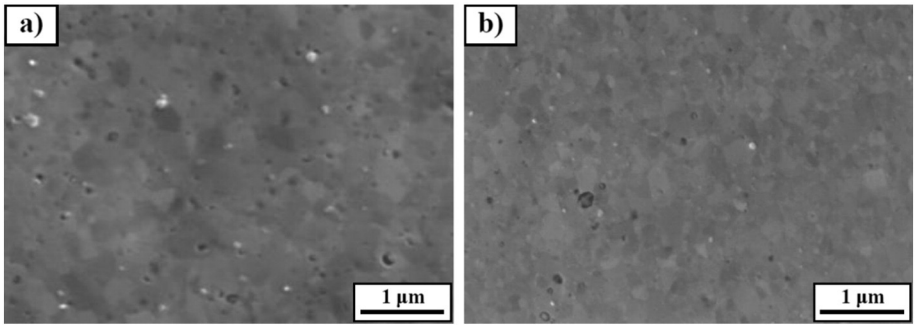

Fig. 3. SEM micrographs of Cu-0.86 at.% Cr alloy after annealing at 550 °C and HPT (a); after annealing at 1000 °C and HPT (b). Small Cr precipitates have a bright contrast in comparison with dark Cu matrix in BSED mode.

alloy. The sample annealed at 1000 °C showed no peaks of Cr particles because of larger dissolution of chromium in the Cu-matrix, but splitting the Cu-peaks was observed in that sample. It indicated low internal stresses and larger grain sizes than those in the sample annealed at 500 °C. The lattice parameters of the Cu-matrix were found to be 3.6179 ± 0.0001 and 3.6164 ± 0.0001 Å for the samples annealed at 500 and 1000 °C, respectively. According to the literature data [22,23], the lattice parameter of Cu decreases as Cr content goes down. Since the dissolution of chromium in the Cu-matrix of the sample annealed at 1000 °C was larger, the lattice parameter was smaller than that in the sample annealed at 500 °C.

The SEM microstructure observation of the samples after HPT showed almost complete dissolution of the large Cr precipitates and partial dissolution of small Cr precipitates in the sample pre-annealed at 550 °C (Fig. 3a). On the other hand, the partial dissolution of large Cr precipitates took place and very small Cr precipitates appeared in the sample pre-annealed at 1000 °C (Fig. 3b). The presence of small precipitates of chromium in the second sample was attributed to the decomposition of the Cu supersaturated solid solution induced by HPT deformation. It should be noted that Cr content in the primary particles was almost two times smaller after deformation then before HPT (Table 1). The concentration of Cr in the small particles was formed due to the decomposition of saturated solid solution was at the same level as in the primary particles after HPT. The reduced content of chromium in the particles after HPT indicated their partial dissolution in the Cu matrix in both samples and a slight enrichment of the matrix with Cr in the sample pre-annealed at 550 °C. Lack of changes in the chemical composition of the matrix in the sample annealed at 1000 °C probably resulted from the interaction of two processes: dissolution of large particles and decomposition of the supersaturated solid solution. The X-ray diffraction measurements of the lattice parameters after HPT correlated well with those data: they reached 3.6151 ± 0.0001 and 3.6163 ± 0.0001 Å for the deformed samples pre-annealed at 550 and 1000 °C, respectively. In other words, the lattice parameter decreased after HPT in the sample pre-annealed at 550 °C (that indicates an increase of Cr content in the Cu-matrix) and did not change in the sample pre-annealed at 1000 °C. The broadening of the XRD pattern peaks from the Cu-matrix was observed in both samples after deformation. It indicated strong grain refinement, which was expected for the HPT, and the appearance of significant microdistortions of the crystal lattice in the deformed material. The TEM observation of microstructure after HPT confirmed the strong grain refinement of the Cu matrix in both samples. Fig. 4 shows the typical bright and dark field TEM micrographs with corresponding selected-area electron diffraction (SAED) of deformed samples. The high density of dislocations was observed inside the Cu phase grains. Some small Cr particles of size about 80 nm were visible in the bright field images. The presence of small Cr particles was also identified using SAED (Fig. 4c, f). The dark field TEM micrographs

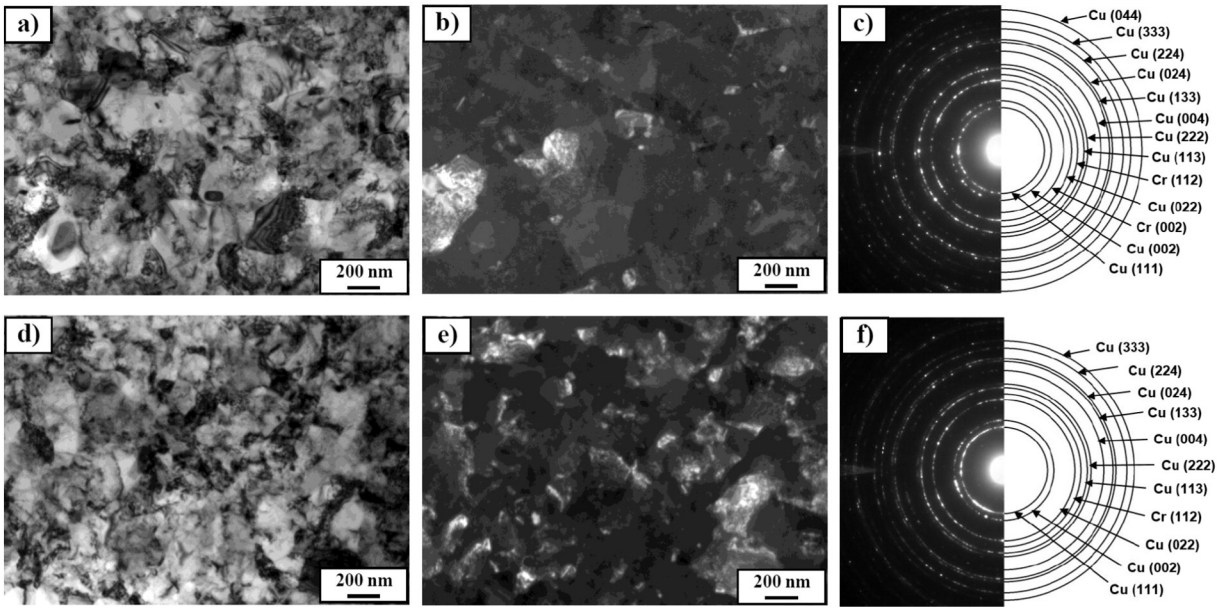

Fig. 4. Bright (a, d) and dark (b, e) field TEM micrographs with corresponding electron diffraction patterns (c, f) of Cu-0.86 at.% Cr alloy after HPT deformation, previously annealed at 550 °C (a–c) and 1000 °C (d–f).

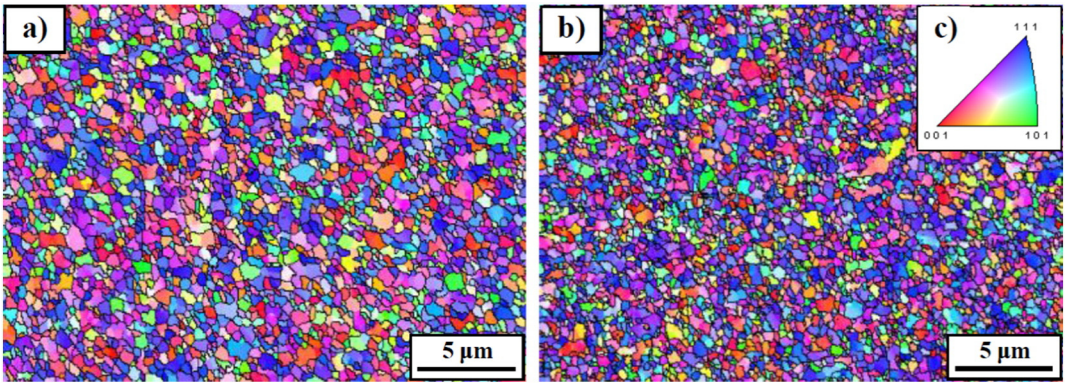

Fig. 5. SEM/EBSD orientation topographies of the Cu-0.86 at.% Cr alloy after HPT deformation, previously annealed at 550 °C (a) and 1000 °C (b), together with standard unit triangle for fcc phase (c). High angle grain boundaries with the misorientation angle between 15 and 65° are marked by black lines.

showed that the grains of Cu phase were characterized mainly by equiaxed form of size about 300–500 nm. The SAED patterns of both samples contained a number of spots which formed almost continuous diffraction rings, which indicated the occurrence of large quantity of small grains with different crystallographic orientation.

A detailed study of the deformed microstructure by the EBSD technique (Fig. 5) showed relatively small fraction of low angle grain boundaries (LAGB) of the copper matrix with the disorientation angle between 4 and 15°: about 8 and 12% for the samples pre-annealed at 550 and 1000 °C, respectively. Their estimated grain sizes were found to be 450 ± 200 and 350 ± 190 nm, respectively. The sample pre-annealed at the higher temperature was characterized by a slightly smaller grain size and a little bit higher fraction of LAGB (all within the measurement error). The analysis of crystallographic texture of the torsion deformed material showed a typical shear texture containing all the fcc shear components. Using the key figure and ODF sections, it can be seen, that the position and maxima of shear components are practically identical for both samples (Fig. 6). Moreover, similar intensities of the components indicate that such an amount of shear ($\gamma = 370$) produces a very homogenous shear texture and does not depend on the initial state. Note, that all the components are slightly deviated from the ideal positions in positive φ_1 direction.

The hardness measurements showed that the hardness of the Cu matrix in the sample annealed at 1000 °C was about 63 $HV_{0.02}$, while the hardness of the Cu matrix with smaller and larger Cr precipitates in the sample annealed at 550 °C was a little bit higher and reached about 70 $HV_{0.02}$. The hardness of the deformed samples measured along the radius is presented in Fig. 7. The hardness value did not change from the center of the samples to their half of radius, and then slightly increased from 142 to 159 and from 159 to 170 for the samples pre-annealed at 550 and 1000 °C, respectively. That indicated that the deformation and thus the microstructure along the radius were almost

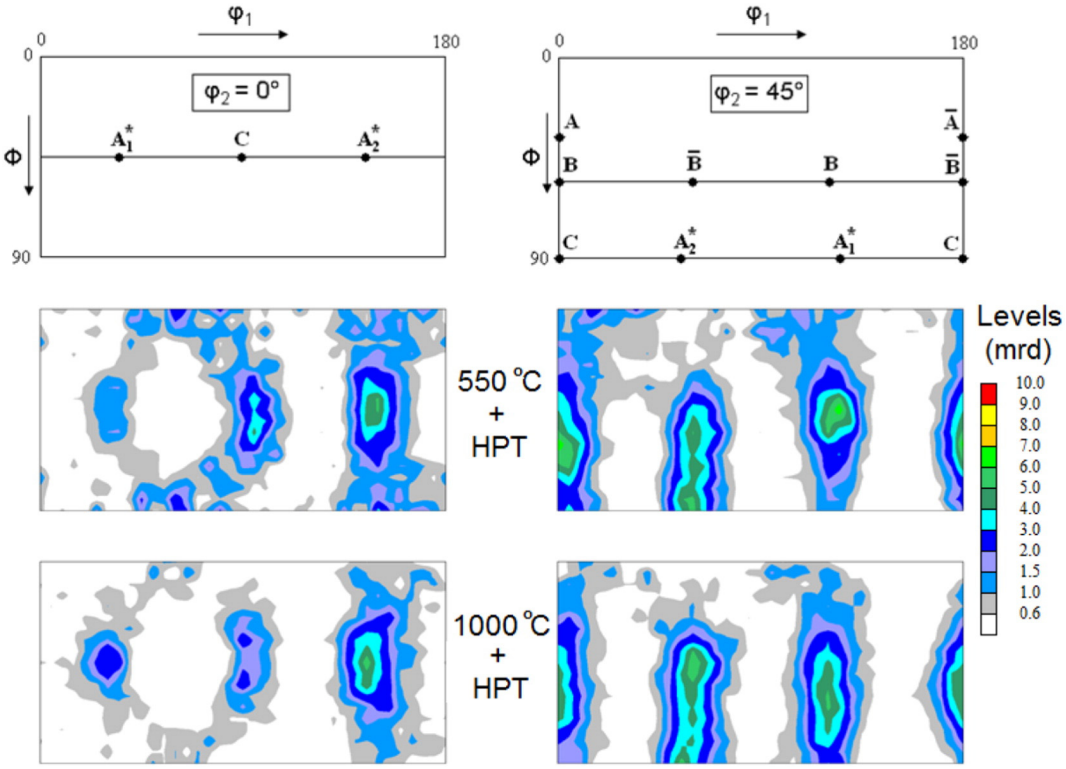

Fig. 6. ODF sections at $\varphi_2 = 0°$ and 45° of the HPT deformed samples at shear strain of about 370 and at room temperatures for two pre-annealing temperatures 550 °C and 1000 °C. Key figure gives the ideal components of simple shear of fcc metal. Intensities are given in multiples of random distribution (mrd).

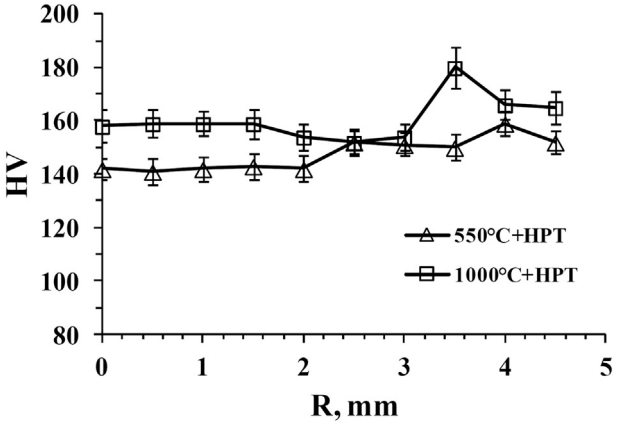

Fig. 7. Changes of hardness measured along radius of the deformed samples.

homogeneous in both samples. The hardness of the deformed sample pre-annealed at 1000 °C was slightly higher than that of the sample pre-annealed at 550 °C. Probably, this was caused by smaller grain sizes and a higher fraction of LAGB. A significant increase of hardness in both deformed samples in comparison with their annealed states was most likely the result of strong grain refinement and increase of dislocation density.

Analyzing the obtained results it can be stated that microstructure of the deformed samples was very similar from the standpoint of grain size, phase composition, texture analysis and hardness measurements. Therefore, it can be concluded that 5 rotations of HPT led to the formation of almost the same structural and phase state in both samples being independent of the initial state.

It is interesting that the severe plastic deformation resulted in the ejection of chromium from the Cu unit cells in the case of supersaturated solid solution (due to the decomposition of this solid solution) and the enrichment of the Cu unit cells with chromium in the case of two phase states due to the dissolution of the second phase (Cr particles). The similar situation was observed in the other copper based alloys subjected to HPT process. For example, the process of decomposition of a supersaturated solid solution after HPT was observed also in the Cu-4.9 wt.% Co alloy pre-annealed at 1060 °C [24] and Cu-77 wt.% Ni alloy pre-annealed at 850 °C [16,25]. The HPT also resulted in a partial dissolution of Co precipitates in the Cu-4.9 wt.% Co alloy pre-annealed at 570 °C. It should be noted that the alloys belonging to Cu—Co, Cu—Ni and Cu—Cr systems are characterized by the positive mixing enthalpy (+10 [26], +11.5 [27] and +12 [28] kJ/mol, respectively), while in the case of alloys with negative mixing enthalpy, for example Cu—In (−5 kJ/mol [29]) the processes of decomposition of saturated solid solution or dissolution of the second phase caused by HPT were very weak [30].

4. Conclusions

High pressure torsion (HPT) of Cu-0.86 at.% Cr alloy resulted in the strong grain refinement of the Cu matrix to go down to about 400 nm in two samples with different initial microstructures. The HPT also resulted in the phase transformations: partial dissolution of Cr precipitates in the sample pre-annealed at 550 °C; dissolution of residual Cr precipitates and weak decomposition of the supersaturated solid solution in the sample pre-annealed at 1000 °C. The crystallographic texture analysis of the deformed samples showed practically identical shear texture for both samples. Similar intensities of the components indicated that the shear texture did not depend on the initial state. The hardness of the deformed sample pre-annealed at 1000 °C was slightly higher than that for the sample pre-annealed at 550 °C, which corresponded to slightly lower grain size in that sample. Finally, it can be concluded that 5 rotations of the HPT led to the formation of almost the same structural and phase state in both samples being independent of the initial state.

Acknowledgements

The authors thank Prof. S. Dobatkin and Dr D. Shangina for useful discussion, and Prof. L. Litińska-Dobrzańska for TEM observations.

All the researches were performed within the Accredited Testing Laboratories with the certificate No. AB 120 issued by the Polish Centre of Accreditation according to European standard PN-ISO/IEC 17025:2005 as well as the EA-2/15.

The work was supported by the National Science Centre of Poland (grant OPUS 2014/13/B/ST8/04247), the Russian Federal Ministry for Education and Science (grants 14.A12.31.0001 and Increased Competitiveness Program of NUST«MISiS») and by the Russian Foundation for Basic Research (grant 15-08-09325).

References

[1] C. Xia, W. Zhang, Z. Kang, Y. Jia, Y. Wu, R. Zhang, G. Xu, M. Wang, High strength and high electrical conductivity Cu–Cr system alloys manufactured by hot rolling–quenching process and thermomechanical treatments, Mater. Sci. Eng. A 538 (2012) 295–301, http://dx.doi.org/10.1016/j.msea.2012.01.047.

[2] J. Stobrawa, L. Ciura, Z. Rdzawski, Rapidly solidified strips of Cu—Cr alloys, Scr. Mater. 34 (1996) 1759–1763, http://dx.doi.org/10.1016/1359-6462(96)00053-X.

[3] X. Wang, J. Zhao, J. He, Investigation on the microstructure and mechanical properties of the spray-formed Cu–Cr alloys, Mater. Sci. Eng. A 460–461 (2007) 69–76, http://dx.doi.org/10.1016/j.msea.2007.01.023.

[4] W. He, E. Wang, L. Hu, Y. Yu, H. Sun, Effect of extrusion on microstructure and properties of a submicron crystalline Cu–5 wt.% Cr alloy, J. Mater. Process. Technol. 208 (2008) 205–210, http://dx.doi.org/10.1016/j.jmatprotec.2007.12.107.

[5] Q. Zhao, Z. Shao, C. Liu, M. Jiang, X. Li, R. Zevenhoven, H. Saxen, Preparation of Cu–Cr alloy powder by mechanical alloying, J. Alloys Compd. 607 (2014) 118–124, http://dx.doi.org/10.1016/j.jallcom.2014.04.054.

[6] Q.J. Wang, Z.Z. Du, L. Luo, W. Wang, Fatigue properties of ultra-fine grain Cu–Cr alloy processed by equal-channel angular pressing, J. Alloys Compd. 526 (2012) 39–44, http://dx.doi.org/10.1016/j.jallcom.2012.02.102.

[7] C.Z. Xu, Q.J. Wang, M.S. Zheng, J.W. Zhu, J.D. Li, M.Q. Huang, Q.M. Jia, Z.Z. Du, Microstructure and properties of ultra-fine grain Cu–Cr alloy prepared by equal-channel angular pressing, Mater. Sci. Eng. A 459 (2007) 303–308, http://dx.doi.org/10.1016/j.msea.2007.01.105.

[8] A. Vinogradov, V. Patlan, Y. Suzuki, K. Kitagawa, V.I. Kopylov, Structure and properties of ultra-fine grain Cu–Cr–Zr alloy produced by equal-channel angular pressing, Acta Mater. 50 (2002) 1639–1651, http://dx.doi.org/10.1016/S1359-6454(01)00437-2.

[9] Y. Ivanisenko, I. MacLaren, X. Sauvage, R.Z. Valiev, H.-J. Fecht, Shear-induced α → γ transformation in nanoscale Fe–C composite, Acta Mater. 54 (2006) 1659–1669, http://dx.doi.org/10.1016/j.actamat.2005.11.034.

[10] S. Ohsaki, S. Kato, N. Tsuji, T. Ohkubo, K. Hono, Bulk mechanical alloying of Cu–Ag and Cu/Zr two-phase microstructures by accumulative roll-bonding process, Acta Mater. 55 (2007) 2885–2895, http://dx.doi.org/10.1016/j.actamat.2006.12.027.

[11] B.B. Straumal, S.V. Dobatkin, A.O. Rodin, S.G. Protasova, A.A. Mazilkin, D. Goll, B. Baretzky, Structure and properties of nanograined Fe–C alloys after severe plastic deformation, Adv. Eng. Mater. 13 (2011) 463–469, http://dx.doi.org/10.1002/adem.201000312.

[12] W. Lojkowski, M. Djahanbakhsh, G. Burkle, S. Gierlotka, W. Zielinski, H.J. Fecht, Nanostructure formation on the surface of railway tracks, Mater. Sci. Eng. A 303 (2001) 197–208, http://dx.doi.org/10.1016/S0921-5093(00)01947-X.

[13] V.V. Stolyarov, R. Lapovok, I.G. Brodova, P.F. Thomson, Ultrafine-grained Al–5 wt.% Fe alloy processed by ECAP with backpressure, Mater. Sci. Eng. A 357 (2003) 159–167, http://dx.doi.org/10.1016/S0921-5093(03)00215–6.

[14] B.B. Straumal, B. Baretzky, A.A. Mazilkin, F. Phillipp, O.A. Kogtenkova, M.N. Volkov, R.Z. Valiev, Formation of nanograined structure and decomposition of supersaturated solid solution during high pressure torsion of Al–Zn and Al–Mg alloys, Acta Mater. 52 (2004) 4469–4478, http://dx.doi.org/10.1016/j.actamat.2004.06.006.

[15] A.A. Mazilkin, B.B. Straumal, E. Rabkin, B. Baretzky, S. Enders, S.G. Protasova, O.A. Kogtenkova, R.Z. Valiev, Softening of nanostructured Al–Zn and Al–Mg alloys after severe plastic deformation, Acta Mater. 54 (2006) 3933–3939, http://dx.doi.org/10.1016/j.actamat.2006.04.025.

[16] B.B. Straumal, S.G. Protasova, A.A. Mazilkin, E. Rabkin, D. Goll, G. Schütz, B. Baretzky, R.Z. Valiev, Deformation-driven formation of equilibrium phases in the Cu–Ni alloys, J. Mater. Sci. 47 (2012) 360–367, http://dx.doi.org/10.1007/s10853-011-5805-0.

[17] A.M. Glezer, M.R. Plotnikova, A.V. Shalimova, S.V. Dobatkin, Severe plastic deformation of amorphous alloys: I. Structure and mechanical properties, Bull. Russ. Acad. Sci. Phys. 73 (2009) 1233–1239.

[18] G.E. Abrosimova, A.S. Aronin, S.V. Dobatkin, S.D. Kaloshkin, D.V. Matveev, O.G. Rybchenko, E.V. Tatyanin, I.I. Zverkova, The formation of nanocrystalline structure in amorphous Fe—Si—B alloy by severe plastic deformation, J. Metastable Nanocryst. Mater. 24 (2005) 69–72, http://dx.doi.org/10.4028/www.scientific.net/JMNM.24-25.69.

[19] X.L. Wang, L. Li, W. Mei, W.L. Wang, J. Sun, Dependence of stress-induced omega transition and mechanical twinning on phase stability in metastable β Ti–V alloys, Mater. Charact. 107 (2015) 149–155, http://dx.doi.org/10.1016/j.matchar.2015.06.038.
[20] Y. Ivanisenko, A. Kilmametov, H. Roesner, R.Z. Valiev, Evidence of α → Ω phase transition in titanium after high pressure torsion, Int. J. Mater. Res. 99 (2008) 36–41, http://dx.doi.org/10.3139/146.101606.
[21] K. Pawlik, P. Ozga, Labotex: the texture analysis software, Göttinger Arbeiten zur Geologie und Paläontologie, SB4:146–147, 1999.
[22] T.P. Harzer, S. Djaziri, R. Raghavan, G. Dehm, Nanostructure and mechanical behavior of metastable Cu–Cr thin films grown by molecular beam epitaxy, Acta Mater. 83 (2015) 318–332, http://dx.doi.org/10.1016/j.actamat.2014.10.013.
[23] A.O. Olofinjanaa, K.S. Tan, Achieving combined high strength and high conductivity in re-processed Cu—Cr alloy, J. Achiev. Mater. Manuf. Eng. 35 (2009) 14–20.
[24] B.B. Straumal, A.R. Kilmametov, Y. Ivanisenko, L. Kurmanaeva, B. Baretzky, Y.O. Kucheev, P. Zięba, A. Korneva, D.A. Molodov, Phase transitions during high pressure torsion of Cu–Co alloys, Mater. Lett. 118 (2014) 111–114, http://dx.doi.org/10.1016/j.matlet.2013.12.042.
[25] B. Straumal, A. Korneva, P. Zięba, Phase transitions in metallic alloys driven by the high pressure torsion, Arch. Civ. Mech. Eng. 14 (2014) 242–249, http://dx.doi.org/10.1016/j.acme.2013.07.002.
[26] C. Gente, M. Oehring, R. Bormann, Formation of thermodynamically unstable solid solutions in the Cu—Co system by mechanical alloying, Phys. Rev. B 48 (1993) 13244, http://dx.doi.org/10.1103/PhysRevB.48.13244.
[27] H.W. Yang, D.P. Tao, Z.H. Zhou, Prediction of the mixing enthalpies of binary liquid alloys by molecular interaction volume model, Acta Metall. Sin. (Engl. Lett.) 21 (2008) 336–340, http://dx.doi.org/10.1016/S1006-7191(08)60056-3.
[28] H.F. Sheng, M. Gong, L.M. Peng, Microstructural characterization and mechanical properties of an $Al_{0.5}$CoCrFeCuNi high-entropy alloy in as-cast and heat-treated/quenched conditions, Mater. Sci. Eng. A 567 (2013) 14–20, http://dx.doi.org/10.1016/j.msea.2013.01.006.
[29] S. Knott, A. Mikula, Calorimetric investigation of the binary Cu—In system, Int. J. Mater. Res. 97 (2006) 1098–1101, http://dx.doi.org/10.3139/146.101343.
[30] B.B. Straumal, A.R. Kilmametov, A.A. Mazilkin, L. Kurmanaeva, Y. Ivanisenko, A. Korneva, P. Zięba, B. Baretzky, Transformations of Cu(in) supersaturated solid solutions under high-pressure torsion, Mater. Lett. 138 (2015) 255–258, http://dx.doi.org/10.1016/j.matlet.2014.10.009.